

Heavy Quarkonia at High Temperature

Jochen Fingberg

*Department of Physics, P.O. Box 10 01 27, University of Wuppertal,
42097 Wuppertal, Germany*

We present a new method to study the properties of heavy quarks at finite temperature. It combines non-relativistic QCD with an improved gluonic action on anisotropic lattices. The efficiency of the approach is demonstrated by the first non-perturbative calculation of the temperature dependence of low-lying quarkonium "pole" masses. For ground state meson masses in the region between charmonium and bottomonium we find only very little variation up to our highest temperature which corresponds to $T \approx 1.2 T_c$ while first excited states indicate a large mass shift.

1 Introduction

At high temperature hadronic matter is expected to undergo a phase transition to the quark-gluon plasma (QGP). In recent years there have been significant theoretical and experimental developments to study its properties. High energy heavy-ion experiments designed to detect spectral changes of hadrons in hot media have already been started. In the search for possible signals of the QGP heavy quarkonium states are among the simplest probes that allow to test the structure of the QCD vacuum. For instance J/Ψ -suppression due to colour screening has been proposed to probe deconfinement [1]. Quarkonium production is rather well understood in hadron-hadron collisions [2]. However, the behaviour of bound states of heavy quarks in a strongly interacting medium close to the deconfinement temperature T_c is still largely uncertain.

Previous theoretical results on the temperature dependence of the masses of the η_c , the J/Ψ , and the Ψ' are not yet completely satisfactory. Different calculations give model dependent results. Some predict a significant decrease [3–6] while others suggest that the masses stay constant [7] or even rise with temperature [8–10]. The assumptions for instance about a temperature dependence of the string tension, $\sigma(T)$, the strong coupling constant, $\alpha_s(T)$, the effective quark mass $M_Q(T)$ and the gluon condensate $\langle \Omega | F_{\mu\nu} F^{\mu\nu} | \Omega \rangle = G^2(T)$ primarily depend on perturbation theory and may not be reliable in the temperature region under consideration.

Progress in numerical simulations of QCD makes reliable predictions about hadronic properties in the non-perturbative regime possible. Recently a non-relativistic approximation of QCD has been used to reproduce the experimental spectrum for heavy quarkonia with high precision [11,12].

At finite temperature a complication arises because Lorentz invariance is explicitly broken so that Green's functions defined by correlators in Euclidean time and space directions are controlled by different phenomena. The heavy quark potential which is confining in the low temperature region becomes Debye-screened at high temperature. On the other hand the pseudo-potential from spatial Wilson loops is confining for all temperatures [13–15]. So far most of the work has been concentrated on the calculation of screening masses obtained from spatial correlators which do not have a direct connection to the physical mass of a resonance as defined for instance by the position of a peak in the spectral function. In recent investigations of the temperature dependent structure in the light mesonic channels screening masses from spatial correlations have been found to differ from effective pole masses from correlations in the Euclidean time direction [9,10]. The mass shift of hadrons made of light quarks is expected to be mainly controlled by chiral symmetry restoration. A realistic simulation would require the inclusion of light dynamical fermions which is expensive. To begin with, it is advantageous to study the temperature dependence of the spectrum with heavy quarks. In this case the influence of light quarks is less important so that a quenched simulation is a reasonable approximation. The binding energy for $c\bar{c}$ (≈ 0.63 GeV) and $b\bar{b}$ (≈ 1.1 GeV) [16] is large compared to the deconfinement temperature $T_c \approx 150 - 250$ MeV. At intermediate temperatures the spectral width of the low lying $q\bar{q}$ bound states is expected to be small so that there will still be a clear distinction between the continuum and the lowest resonance. The binding energy of quarkonia decreases with temperature. The dissociation temperature of the (Υ , Υ') is expected to be in the region of $T \approx (2.6, 1.1) T_c$ [17]. However, these values still contain a model dependent uncertainty.

Our approach is based on an improved gluonic action for the light degrees of freedom and a non-relativistic formalism (NRQCD) for the heavy quarks [18]. Finite temperature NRQCD (FT-NRQCD) uses anisotropic lattices [19–21] to achieve a finer resolution in time direction. A large number of Matsubara frequencies is necessary to accurately measure temporal meson propagators. The problem is first approached in quenched QCD by considering a quark-antiquark pair propagating in Euclidean time direction in a gluonic medium. To show the feasibility of the new approach and the significance of its results we calculate temporal meson correlators for bare quark masses between 2 and 6 GeV.

2 Heavy meson spectrum at finite temperature

Heavy quarkonia are small and tightly bound. We know that asymptotically for infinite quark mass a potential picture will give the correct description. The Cornell potential

$$V(r) = \sigma r - \frac{\alpha_s}{r} \quad (1)$$

reproduces the experimental spectrum for charmonium and bottomonium quite well. In a thermal medium of temperature $T > 0$ the potential is modified by colour screening which can be parameterized in the form [22]

$$V_T(r) = \frac{\sigma}{\mu(T)}(1 - \exp(-\mu(T)r)) - \frac{\alpha_s}{r} \exp(-\mu(T)r) \quad . \quad (2)$$

Eq. 2 is equivalent to the Cornell form with a temperature dependent string tension $\sigma(T) = \sigma/(\mu(T)r)(1 - \exp(-\mu(T)r))$ and a screened Coulomb term $\alpha_s(T) = \alpha_s \exp(-\mu(T)r)$. From fig. 1a we see that $V_T(r)$ changes differently

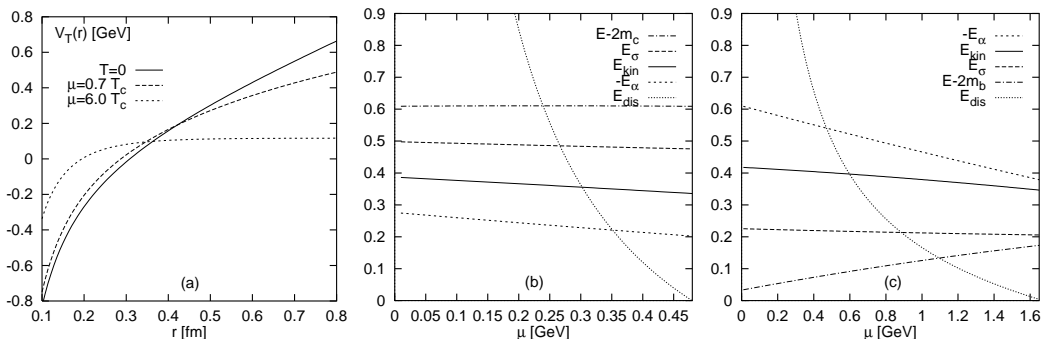


Fig. 1. The heavy quark potential (a) as a function of the radius for 3 different temperatures and the terms contributing to the total energy together with the dissociation energy in GeV as a function of the Debye-mass for $c\bar{c}$ (b) and $b\bar{b}$ (c).

with temperature for small $r < 0.3$ fm and large $r > 0.4$ fm. The temperature dependence is entirely contained in the Debye-mass. It has been argued [23] that due to string breaking $\mu(T)$ will be different from zero even for $T = 0$ and that the effective string tension does not vanish immediately above T_c modeling non-perturbative interactions in the plasma. Although the precise functional dependence is not very well known the string tension and the strong coupling will decrease when the temperature and thereby $\mu(T)$ is increased.

First qualitative insight in the behaviour of $Q\bar{Q}$ -states can be obtained from a semi-classical picture [23]. As a consequence of the uncertainty relation which forces $\langle p^2 \rangle \langle r^2 \rangle \approx 1$ the kinetic energy, $E_{kin} = p^2/m \approx 1/mr^2$, decreases with the quark separation. Minimizing the total Energy, $E(r) = 2m + E_{kin} + V$, the

ground state is found where the decrease of the kinetic energy is compensated by an increase of the potential energy. The result is that the binding radius $r_0(\mu)$ increases with $\mu(T)$. A minimum of $E(r)$ exists as long as the screening is not too strong. The meson will dissociate once the Debye-mass $\mu(T)$ becomes larger than a critical value μ_c . Below this value the meson mass depends on the temperature. In general the sign and the magnitude of the mass shift, $\Delta M = M(T) - M(T = 0)$, depend on the details of the balance of potential (Coulomb and string) and kinetic energy as is shown in figs. 1b and c. In the potential of eq. 2 masses can decrease or increase with T depending on the size of the $Q\bar{Q}$ bound state.

Understanding the basic mechanism in the semi-classical approximation we can move towards a quantitative understanding and calculate quarkonium wave-functions in a non-relativistic potential model. The mean quark velocity can be computed from averages obtained by a numerical solution of the Schrödinger equation with a potential of the form given in eq. 2,

$$\langle v^2 \rangle_T = \frac{E(T) - \sigma(T)\langle r \rangle_T + \alpha_s(T)\langle 1/r \rangle_T}{M} \quad (3)$$

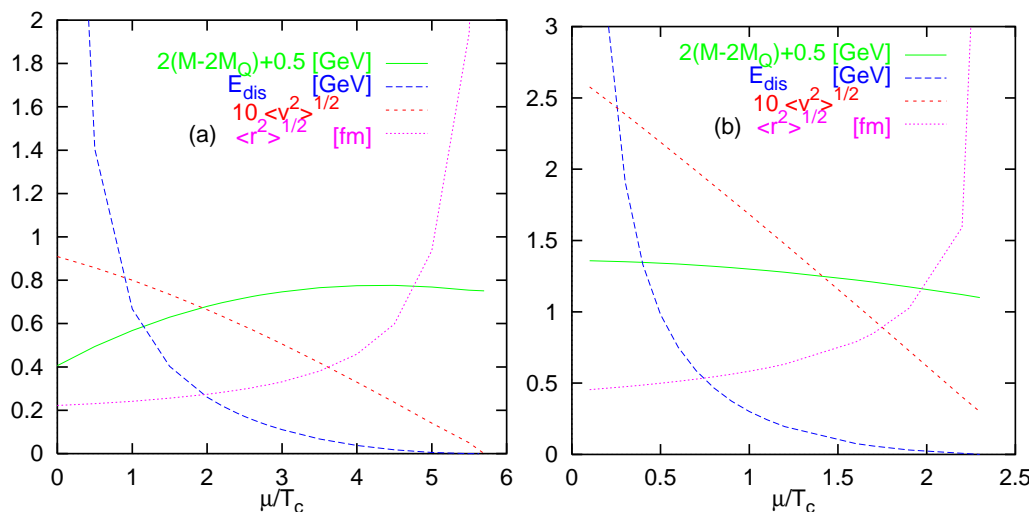


Fig. 2. Dependence of the velocity, radius, mass and dissociation energy in the (1S) state on the Debye-mass for $b\bar{b}$ (a) and $c\bar{c}$ (b). The velocity and the meson mass have been rescaled to fit in the same frame.

From fig. 2 we see that the average quark velocity decreases with temperature so that a non-relativistic ansatz for the heavy degrees of freedom seems to be justified for $T > 0$.

However, beyond this simple potential picture we know that lattice data do not agree very well with the perturbative expectation for the form of the heavy quark potential at least up to $T \leq 4 T_c$ [24–26]. A precise measurement of the Debye-mass is plagued by ambiguities in the form of the function used to fit

the heavy quark potential.

Lattice simulations can provide a reliable determination of the meson spectrum without assumptions about the heavy quark potential. Thus, it is important to compare phenomenological and numerical results to gain further insight in the structure of the QCD vacuum at finite temperature.

Compared to zero temperature additional care is necessary because any excitation acquires a finite lifetime at non-zero temperature [27]. The spectral function $\rho(p, \omega)$ of an excitation with momentum p and energy ω which is a δ -function at $T = 0$ will broaden. This effect will modify the meson propagator, $G_m(t)$.

3 FT-NRQCD

We can go beyond a potential model approximation and calculate the action of heavy quarks in a gluonic heat-bath from first principles. The proposed method is based on the formalism of non-relativistic QCD [18] and a discretization of quantum field theories at finite temperature on anisotropic lattices [19–21]. NRQCD is an effective theory that has been successfully applied to bottomonium and charmonium at zero temperature [11,12]. It allows an efficient and accurate calculation of heavy quark propagators. At zero temperature the binding energy of a $b\bar{b}$ -system can be estimated from its distance to the open b threshold, $E_b = M_{b\bar{b}} - 2m_B \approx 1.1$ GeV. The binding energy is large compared to the deconfinement temperature, $T_c \approx 150 - 250$ MeV, so that we expect a smooth evolution of the system away from its ground state at $T = 0$ as the temperature is increased. From previous considerations of potential models we expect the average quark velocity to decrease with temperature so that there will be a range of temperatures $T > 0$ where FT-NRQCD is applicable.

The total action for a system of heavy quarks in a gluonic heat-bath naturally splits into a relativistic part for the gluons and a non-relativistic term for the heavy quarks.

$$S = S_R + S_{NR} \tag{4}$$

The relativistic simulations use a tree-level improved gauge action [28,29] with a plaquette and a rectangle term on asymmetric lattices with separate spatial coupling β_σ and temporal coupling β_τ .

$$\begin{aligned}
S_R = & \beta \left[\gamma^{-1} \sum_{x, 4>\nu>\mu} \left((1 - \nu \square_{x\mu}) - c_\sigma (1 - \nu \square_{x\mu}^{\text{top}}) - c_\sigma \left(1 - \nu \square_{x\mu}^{\text{right}} \right) \right) \right. \\
& + \gamma \sum_{x, 4=\nu>\mu} \left(\frac{u_\sigma^2}{u_\tau^2} (1 - \nu \square_{x\mu}) - c_\tau (1 - \nu \square_{x\mu}^{\text{top}}) - c_\tau \frac{u_\sigma^2}{u_\tau^2} \left(1 - \nu \square_{x\mu}^{\text{right}} \right) \right) \left. \right] \quad (5) \\
c_\sigma = & \frac{1}{20 u_\sigma^2}, \quad c_\tau = \frac{1}{20 u_\tau^2}
\end{aligned}$$

The asymmetry parameter $\gamma = \sqrt{\beta_\tau/\beta_\sigma}$ and the coupling $\beta = \sqrt{\beta_\tau \beta_\sigma}$ are defined in terms of the spatial coupling β_σ and the temporal coupling β_τ . In principle, tadpole improvement can be implemented by factors

$$u_\sigma = \left\langle \frac{1}{3} \text{Re Tr } \square_{\sigma\sigma} \right\rangle^{1/4} \quad \text{and} \quad u_\tau = \left\langle \frac{1}{3} \text{Re Tr } \square_{\sigma\tau} \right\rangle^{1/4}$$

which can be calculated from the average spatial and temporal plaquette as indicated or the mean link in Landau gauge. The anisotropy $\xi = a_\sigma/a_\tau > 1$ becomes equal to the asymmetry parameter γ only in the continuum limit, $\beta \rightarrow \infty$. At finite gauge coupling, they differ by a renormalization factor $\eta = \xi/\gamma$ which can be determined nonperturbatively in a calibration procedure. The additional parameter γ allows to have a large number of lattice points in time direction while keeping the temperature $T = (N_\tau a_\tau)^{-1} = (N_\tau \xi a_\sigma)^{-1}$ fixed.

The non-relativistic action is derived from the Dirac equation by a Foldy-Wouthuysen transformation. The resulting effective field theory called NRQCD approximates relativistic QCD at small energies. Relativistic heavy-quark momenta are excluded from the theory by choosing a spatial lattice spacing $a_\sigma^{-1} \simeq M_Q$. The $1/M_Q$ expansion underlying the formalism of NRQCD will hold as long as the average quark velocity is small, $v \ll 1$. The non-relativistic action has the form

$$S_{NR} = \Psi^\dagger (D_t + H_0 + \delta H) \Psi \quad (6)$$

where D_t denotes the covariant time derivative, H_0 is the kinetic energy operator and δH is the leading relativistic and finite-lattice-spacing correction. Here we include all spin-independent relativistic corrections to order $M_Q v^4$ and spin-dependent corrections to order $M_Q v^6$. Modifications to the corresponding form of S_{NR} for $T = 0$ as given in ref. [30] appear only in the correction δH where the improved temporal derivative and the chromoelectric field strength introduce additional factors of ξ . To simplify matters, tadpole improvement of S_{NR} was implemented only for spatial links. In our case the spatial lattice spacing is considerably larger than the temporal spacing so that the mean

temporal link u_τ is very close to unity [21].

The heavy quark propagators are computed using the evolution equation

$$G_{t+a_\tau} = \left(1 - \frac{a_\tau H_0}{2}\right) U_4^\dagger \left(1 - \frac{a_\tau H_0}{2}\right) (1 - a_\tau \delta H) G_t \quad (7)$$

The non-relativistic quark propagator is not periodic in time and can be evaluated at times larger than $N_\tau/2$. A symmetric (antisymmetric) propagator can be constructed by explicitly adding (subtracting) the contributions from mirror charges. On a Euclidean lattice at temperature $T = 1/(a_\tau N_\tau)$ thermal Green's functions can be evaluated only on a discrete set of frequencies $\omega_n = 2\pi nT$, $n = 1 \dots N_\tau$. It is obvious that a good resolution requires a large number of grid points in temperature direction. Thermal meson states

$$G_m(p, t) = \sum_x \text{Tr} \left[\sum_r G_t^\dagger(x-r) \Gamma^{(sk)}(r) \sum_s G_t(x-s) \Gamma^{(sc)}(s) \right] e^{ipx} \quad (8)$$

corresponding to 3S_1 and 1S_0 -states were constructed from the quark propagators. Interpolating operators of the form $\Gamma(r) = \Omega^{spin} \Phi(r)$ with 11 different combinations of local and smeared trial wave-functions at the source and sink were used. The wave-functions were determined solving the Schrödinger equation for a Breit-Fermi potential [31] for each value of the bare quark mass. The same set of wave-functions was used for all temperatures.

4 Simulation details and results

For the relativistic simulations we choose an asymmetry parameter $\gamma = 4$ so that our largest lattice size, $16^3 \times 64$ corresponds to a symmetric lattice at zero temperature. The temperature was varied by reducing the value of N_τ from 64 to 24 and 16 for fixed spatial lattice size, $N_\sigma = 16$. The value of the bare coupling, $\beta = 4.31466$, corresponds to the critical coupling $\beta_{\text{Wilson}} = 5.8941$ [32,33] for $\gamma = 1$ on a lattice with $N_\tau^{\text{critical}} = 6$. In this way it is possible to get a rough estimate of the spatial lattice spacing from the string tension $\sqrt{\sigma}a = 0.2734(37)$ at $\beta_{\text{Wilson}} = 5.8941$ [33]. We expect the inverse spatial lattice spacing to be in the region $a_\sigma^{-1} = \sqrt{\sigma}/0.2734 \approx 1.5$ GeV. However, a value of $\gamma \neq 1$ will modify this correspondence and change the value of the spatial lattice spacing. The remaining free parameter, the bare quark mass, was varied in the range $a_\sigma M_Q = 1.5, 2, 2.5, 3, 3.5, 4$. After generating ≈ 100 independent gauge field configurations we determined zero momentum meson propagators for 1S_0 and 3S_1 states. For local 1S_0 states we also measured finite momentum propagators.

Before we can measure the meson spectrum we have to determine the asymmetry $\xi = a_\sigma/a_\tau$ and set the scale a_σ . The heavy quark potential at $T = 0$ can be measured either from spatial or temporal Wilson loops. The asymmetry parameter is determined in a calibration procedure from spatial and temporal potential differences. The parameter ξ can be calculated most accurately at

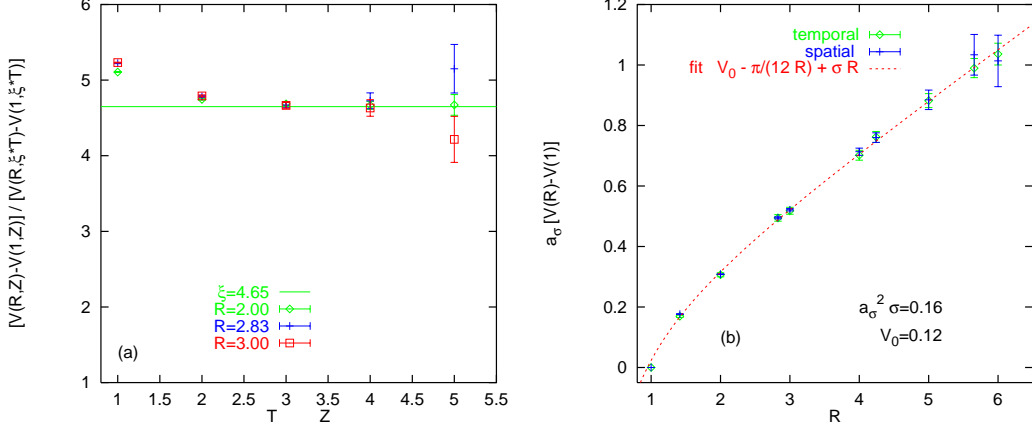


Fig. 3. The ratio of spatial and temporal potential differences (a) and heavy quark potential from temporal and spatial Wilson loops (b).

small distances where the statistical error is small. In fig. 3a we see that for the smallest separation $R = 2$ the ratio of potential differences agrees with $\xi = 4.65$ for all separations $T > 2$. All values for larger separations $R = 2.83$ and $R = 3$ are in accord with this value within the statistical errors. Fig. 3b shows that spatial and temporal Wilson loops give the same physical potential when this value of the asymmetry parameter is used. Knowing ξ and $a_\sigma\sqrt{\sigma}$ an estimate of the temperature can be obtained from the relation

$$\frac{T}{T_c} = \frac{T}{\sqrt{\sigma}} \frac{\sqrt{\sigma}}{T_c} = \frac{\xi}{N_\tau(a_\sigma\sqrt{\sigma})(T_c/\sqrt{\sigma})} \approx \frac{19}{N_\tau} \approx 0.8, 1.2 \quad (N_\tau = 24, 16) \quad ,$$

where we use a value of $T_c/\sqrt{\sigma} = 0.625$ [33]. A least squares fit to the static potential with the functional form $V(R) = V_0 - \pi/(12R) + \sigma R$ gives the result $a_\sigma^2\sigma = 0.16$. This translates to $a_\sigma^{-1} \approx 1.1$ GeV when the phenomenological value for the string tension, $\sqrt{\sigma} = 427$ MeV, is used. To show the consistency a second estimate for the spatial lattice spacing is determined from the hyperfine splitting of the ground state, ΔE_{hyp} . Two conditions are needed to fix the unknown parameters a_σ^{-1} and M_Q . First we set the scale and determine a_σ^{-1} from $M_{kin} = M_{\eta_b} = M_\Upsilon - \Delta E_{hyp}$ where we use the experimental value for the mass of the $\Upsilon(1S) = 9.46037(21)$ GeV [16]. The kinetic mass M_{kin} is determined from a fit to a non-relativistic dispersion relation,

$$M(p) = M_1 + \frac{|P|^2}{2M_{kin}} + \dots \quad (9)$$

Table 1

The kinetic mass and hyperfine splitting of the ground state for various values of the bare quark mass for $\xi = 4.65$ and ΔE_{hyp} between 15 and 25 MeV.

$a_\sigma M_Q$	$\xi a_\sigma M_{kin}$	$a_\sigma^{-1} = \frac{\xi M_{\eta_b}}{\xi a_\sigma M_{kin}}$	$a_\tau \Delta E_{hyp} = \frac{\Delta E_{hyp}}{\xi a_\sigma^{-1}}$
1.5	15.4 (2)	2.85 GeV	0.0011 – 0.0019
2.0	20.1 (3)	2.18 GeV	0.0015 – 0.0025
2.5	24.8 (4)	1.77 GeV	0.0018 – 0.0030
3.0	29.6 (5)	1.48 GeV	0.0022 – 0.0036
3.5	34.5 (7)	1.27 GeV	0.0025 – 0.0042
4.0	39.8 (10)	1.10 GeV	0.0029 – 0.0049

where $M(p)$ is the mass extracted from finite momentum propagators. From previous calculations ΔE_{hyp} is expected to be in the region between 15 and 25 MeV at our presumably large value of a_σ^{-1} between 1.1 and 1.5 GeV [34].

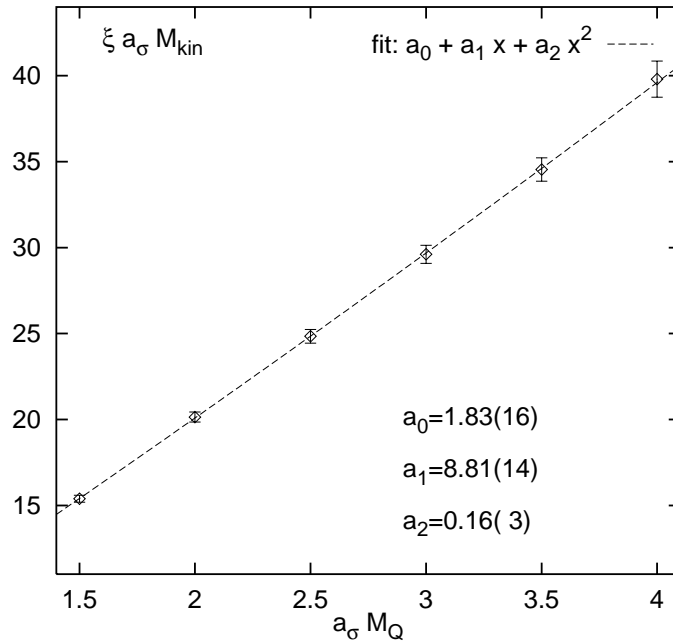


Fig. 4. The kinetic mass of the 1S_0 meson as a function of the bare quark mass.

The value of $a_\sigma^{-1} = \xi M_{\eta_b} / (\xi M_{kin})$ is used to compare the expected ΔE_{hyp} with the measured $^3S_1 - ^1S_0$ splitting. From figs. 5 we see that the best agreement is achieved for $M_Q = 3.5$ which corresponds to $a_\sigma^{-1} \approx 1.3$ GeV. There is a 15% difference between this value and the estimate from the string tension. Both values are consistent within the expected accuracy. A discrepancy of this size has also been found in NRQCD studies at $T = 0$ [35]. A more stringent test and a better determination of a_σ will be possible once the $1S - 1P$ splitting has been measured [36].

The easiest quantities to calculate are 1S_0 propagators for point sources. Scaled propagators, $H(T) = G(T)/G(T = 0)$, show directly the changes in the spectrum due to the temperature. The zero point energy which in principal can be computed using weak coupling perturbation theory is the same for all three temperatures because we vary only N_τ keeping all other parameters fixed. The mass shift $\Delta M(T) = M_{meson}(T) - M_{meson}(T = 0)$ can be extracted from the slope of the scaled propagator at large time steps. A positive slope indicates an increase while a negative slope will be seen if masses decrease with temperature.

Our numerical results show that the signal for $Q\bar{Q}$ bound states persists to high temperature, $T \approx 1.2 T_c$. Compared to $T = 0$ the ground state meson propagators change very little. The observed temperature dependence of the scaled propagator (fig. 6) is weak. Looking at it in more detail we see that the ground state meson mass decreases with T . Fig. 6 shows the scaled propagators for $N_\tau = 16$ and 24. The scale is logarithmic and we expect a linear form for an exponential behaviour, $G(t) \propto \exp(-\Delta M t)$. For $N_\tau = 24$ which corresponds to $T \approx 0.8 T_c$ the scaled propagator agrees with unity. It does not show any significant change with temperature in the entire mass range, $1.5 \leq a_\sigma M_Q \leq 4$. For $N_\tau = 16$ which corresponds to a temperature $T \approx 1.2 T_c$ we observe a clear increase of the scaled propagator with Euclidean time. This signals a broadening of the spectral function and is an indication of a possible decrease of the effective meson mass at this value of the temperature. As expected, the effect becomes weaker as we go to larger quark mass. To illustrate the order of magnitude we included a straight line in fig. 6 which corresponds to a small shift of $-\Delta M = a_\tau^{-1}(\ln 1.06)/6 \approx 12$ MeV. It is important to note that we used point sources and sinks which do not distort the spectral function. The observed effect is a signal that the mixture of states excited by the local source gets broader and possibly lighter with increasing temperature. If there is no cancellation in the sense that the ground state gets heavier while higher excitation become lighter then particularly the ground state mass will decrease with temperature.

It is expected that first excited states dissociate immediately above the phase transition. In fig. 7 we see no effect at $T \approx 0.8 T_c$ but a strong increase of the propagators at $T \approx 1.2 T_c$. Compared to the ground state the increase is much stronger so that it seems likely that the first excited state is dissociated at this temperature. Again, the order of magnitude of the effect is illustrated in fig. 7 by a straight line which now corresponds to a shift of $-\Delta M = a_\tau^{-1}(\ln 3)/10 \approx 240$ MeV. Since there is no local operator projecting on the first excited state this result has been obtained with a smeared source and sink. The trial wave-function can only approximate the temperature wave-function causing a possible residual distortion of the quarkonium propagator. To overcome this problem a measurement of the temperature wave function is desirable [36].

Our numerical results can be contrasted with an expectation from the density matrix formalism. If we assume that the thermal meson state consists of a mixture of zero temperature states with a statistical weight given by the Boltzmann factor $G(t, T) = \sum_i \exp(-M_i/T) \exp(-M_i t)$ then we would expect a decrease of the scaled propagator with t because more and more heavier states contribute as the temperature is increased. The observed increase of the scaled propagators cannot be explained by a simple temperature dependent admixture of higher mesonic states with negligible spectral width.

5 Summary

We have performed a first non-perturbative study of the heavy meson spectrum and dispersion relation at finite temperature using FT-NRQCD. We found no change in the spectrum for temperatures below the deconfinement transition and strong non-trivial effects above T_c .

A comparison of S-state meson propagators at $T = 0$ and $T \approx 0.8 T_c$ showed no significant differences in the entire Euclidean time range, $t \leq 16$. The local operator used for the ground state does not distort or re-weight the spectral function. At low time steps it gets contributions not only from the ground state but also from higher excitations. If this quantity is unchanged at large t so is the true ground state.

A further increase of the temperature to $T \approx 1.2 T_c$ showed a clear signal for a broadening of the spectral function of the ground state. This can be interpreted as an indication for a small decrease of the meson mass with temperature. The phenomenon is stronger the lighter the quark mass is. As expected we see that the first excited S-state is more susceptible to the temperature. Across the deconfinement transition we observe a strong change between $T \approx 0.8 T_c$ and $T \approx 1.2 T_c$. This can be taken as a first indication for the dissociation of these states.

Qualitatively all our observations are in accord with the expectations from the phenomenological picture of Debye-screening in a potential model. The heavier the mesons the smaller they are and the less they feel the screening. This has important implications for the deconfinement transition. The confined degrees of freedom are not released at a single temperature T_c but the transition to a quark gluon plasma proceeds in steps. The determination of the dissociation temperature of different bound states of heavy quarks is an interesting problem which deserves further efforts [36].

There is a discrepancy with other models that predict a strong effect already below $T \leq T_c$ such as a weakening of $\sigma(T)$. The string tension surely has

to vanish at $T = T_c$. However, this effect is a long range phenomenon. At smaller distances remaining strong interactions can still give rise to an effective string tension $\sigma(R, T) > 0$. Furthermore, we see only a small change of the ground state mass up to $T = 1.2 T_c$ unlike predicted by most phenomenological models. A crossover between a behaviour dominated by the strong coupling constant at small distances and the string tension at larger separations is not observed in the accessible mass range. This gives further support to the observation that the perturbative form of the heavy quark potential is wrong in the temperature range under consideration.

A precise measurement of the shift of the meson mass at higher temperature requires further work [36]. For the future we intend to measure the wavefunction and use it to improve the ground-state overlap of our operators. We expect that a multi-state fit with the improved operators allows a determination of the spectrum at higher temperature.

6 Acknowledgments

We thank Frithjof Karsch, Helmut Satz and Edwin Laermann for useful conversations and the SESAM-collaboration for continuous support. The computations were done on the Quadrics Q4 and the Connection Machine CM2 in Wuppertal. J.F. thankfully acknowledges a fellowship from the Deutsche Forschungsgemeinschaft.

References

- [1] T.Matsui and H.Satz, Phys. Lett. B178 (1986) 416.
- [2] A. Sansoni et al. (CDF Collaboration), *Quarkonia Production at CDF*, FERMILAB-CONF-96-221-E; E. Braaten, Nucl. Phys. A610 (1996) 386c; M.L. Mangano, CERN-TH/95-190; M.L. Mangano and A. Petrelli, e-Print Archive: hep-ph/9610364.
- [3] T. Hashimoto, O. Miyamnura, K. Hirose and T. Kanki, Phys. Rev. Lett. 57 (1986) 2123.
- [4] T. Hashimoto, K. Hirose, T. Kanki, O. Miyamura, Z. Phys. C38 (1988) 251.
- [5] S. Hioki, T. Kanki and O. Miyamura, Prog. Theor. Phys. 85 (1991) 603.
- [6] R.J. Furnstahl, T. Hatsuda and S.H. Lee, Phys. Rev. D42 (1990) 1744.
- [7] F.O. Gottfried and S.P. Klevansky, Phys. Lett. B286 (1992) 221.
- [8] F.S. Navarra and C.A.A. Nunes, Phys. Lett. B356 (1995) 439.

- [9] T. Hashimoto, A. Nakamura and I.O. Stamatescu, Nucl. Phys. B400 (1993) 267; Nucl. Phys. B406 (1993) 325.
- [10] K. Akemi et al. (QCD-Taro collaboration), Nucl. Phys. B (Proc. Suppl.) 42 (1995) 445; M. Fujisaki et al. (QCD-Taro collaboration), Nucl. Phys. B (Proc. Suppl.) 53 (1997) 426,
- [11] C.T.H. Davies et al., Phys. Rev. D50 (1994) 6963.
- [12] C.T.H. Davies et al., Phys. Rev. D52 (1995) 6519.
- [13] E. Manousakis and J. Polonyi, Phys. Rev. Lett. 58 (1987) 847.
- [14] G. Bali, J. Fingberg, U.M. Heller, F. Karsch and K. Schilling, Phys. Rev. Lett. 71 (1993) 3059.
- [15] F. Karsch, E. Laermann and M. Lütgemeier, Phys. Lett. B346 (1995) 94.
- [16] R.M. Barnett et al. (Particle Data Group), Phys. Rev. D54 (1996) 1.
- [17] F. Karsch and H. Satz, Z. Phys. C51 (1991) 209.
- [18] G.P. Lepage and B.A. Thacker, Phys. Rev. D43 (1991) 196; K. Hornbostel, G.P. Lepage, L. Magnea, U. Magnea and C. Nakhleh, Phys. Rev. D46 (1992) 4052.
- [19] F. Karsch, Nucl. Phys. B205 (1982) 285.
- [20] G. Burgers, F. Karsch, A. Nakamura and I.O. Stamatescu, Nucl. Phys. B304 (1988) 587.
- [21] C. Morningstar, Nucl. Phys. Proc. Suppl. 53 (1997) 914; e-Print Archive: hep-lat/9704011.
- [22] H. Joos and I. Montvay, Nucl. Phys. B225 (1983) 565.
- [23] F. Karsch, M.T. Mehr and H. Satz, Z. Phys. C37 (1988) 617.
- [24] E. Laermann, Nucl. Phys. B (Proc. Suppl.) 42 (1995) 120.
- [25] B. Petterson, Nucl. Phys. A525 (1991) 237.
- [26] L.I. Unger, Phys. Rev. D48 (1993) 3319.
- [27] P.A. Henning, Phys. Rep. 253 (1995) 235.
- [28] M. García Pérez, J. Snippe and P. van Baal, *Testing Improved Actions*, e-Print Archive: hep-lat/9607007.
- [29] M. García Pérez and P. van Baal, Phys. Lett. B392 (1997) 163.
- [30] C. Morningstar, Phys. Rev. D50 (1994) 5902.
- [31] G. Bali, K. Schilling and A. Wachter, *Complete $O(v^2)$ corrections to the static interquark potential from $SU(3)$ gauge theory*, e-Print Archive: hep-lat/9703019.

- [32] G. Cella, G. Gurci, A. Vicere and B. Vigna, Phys. Lett. B333 (1994) 457.
- [33] G. Boyd, J. Engels, F. Karsch, E. Laermann, C. Legeland, M. Lütgemeier and B. Petersson, Nucl. Phys. B469 (1996) 419.
- [34] C.T.H. Davies, *The Spectrum from Lattice NRQCD*, e-Print Archive: hep-lat/9705039.
- [35] S. Collins et al., Phys. Rev. D54 (1996) 5777.
- [36] J. Fingberg, work in progress.

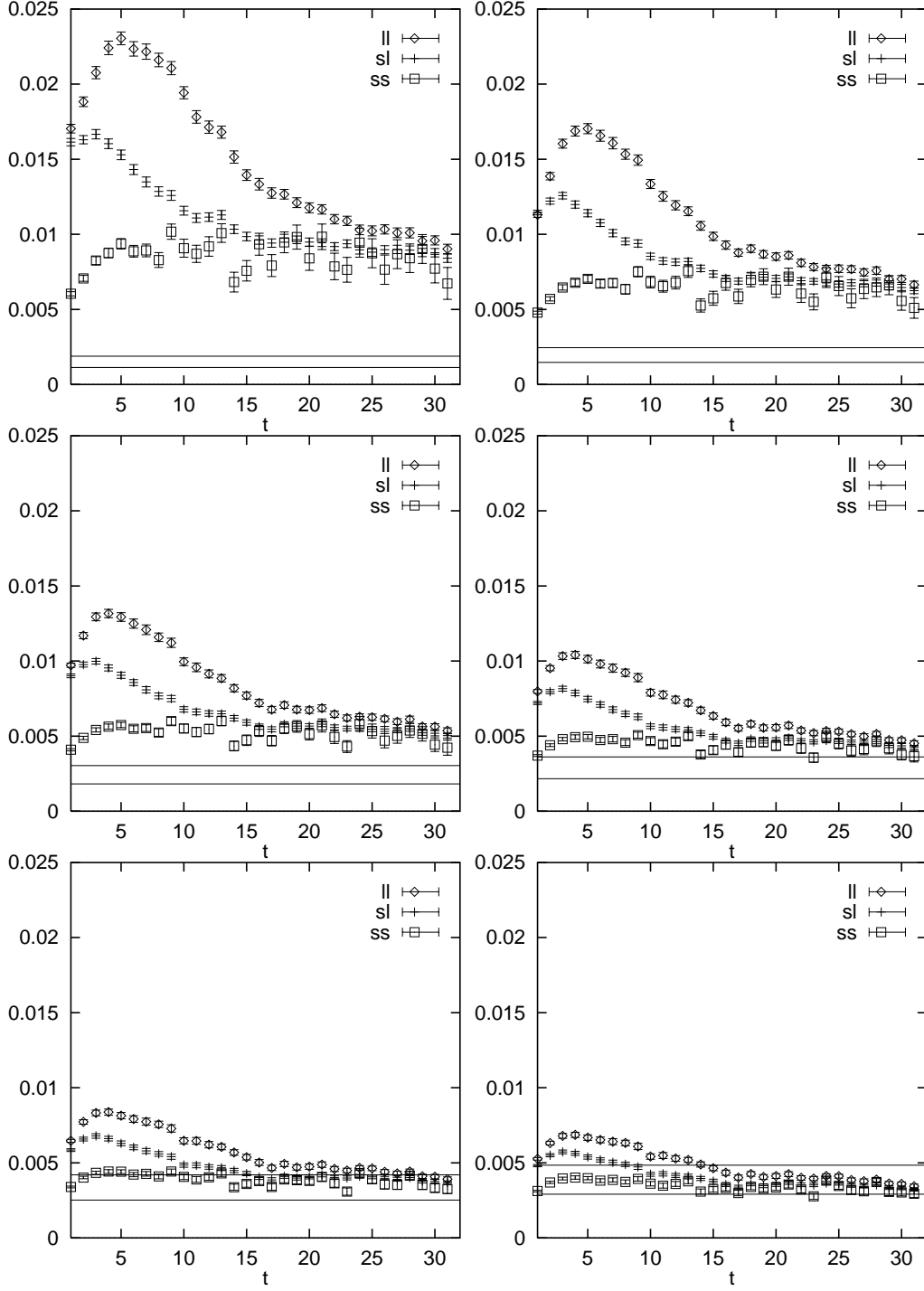


Fig. 5. Local masses $\ln(G_m(t)/G_m(t+a_\tau))$ for the $^1S_0 - ^3S_1$ splitting in units of a_τ^{-1} from local-local (ll), smeared-local (sl) and smeared-smeared (ss) propagators compared with the expectation obtained from $\Delta E = 15 - 25$ MeV. We start with the lowest bare quark mass $a_\sigma M_Q = 1.5$ in the upper left corner and go in intervals of 0.5 to the lower right corner with $a_\sigma M_Q = 4.0$.

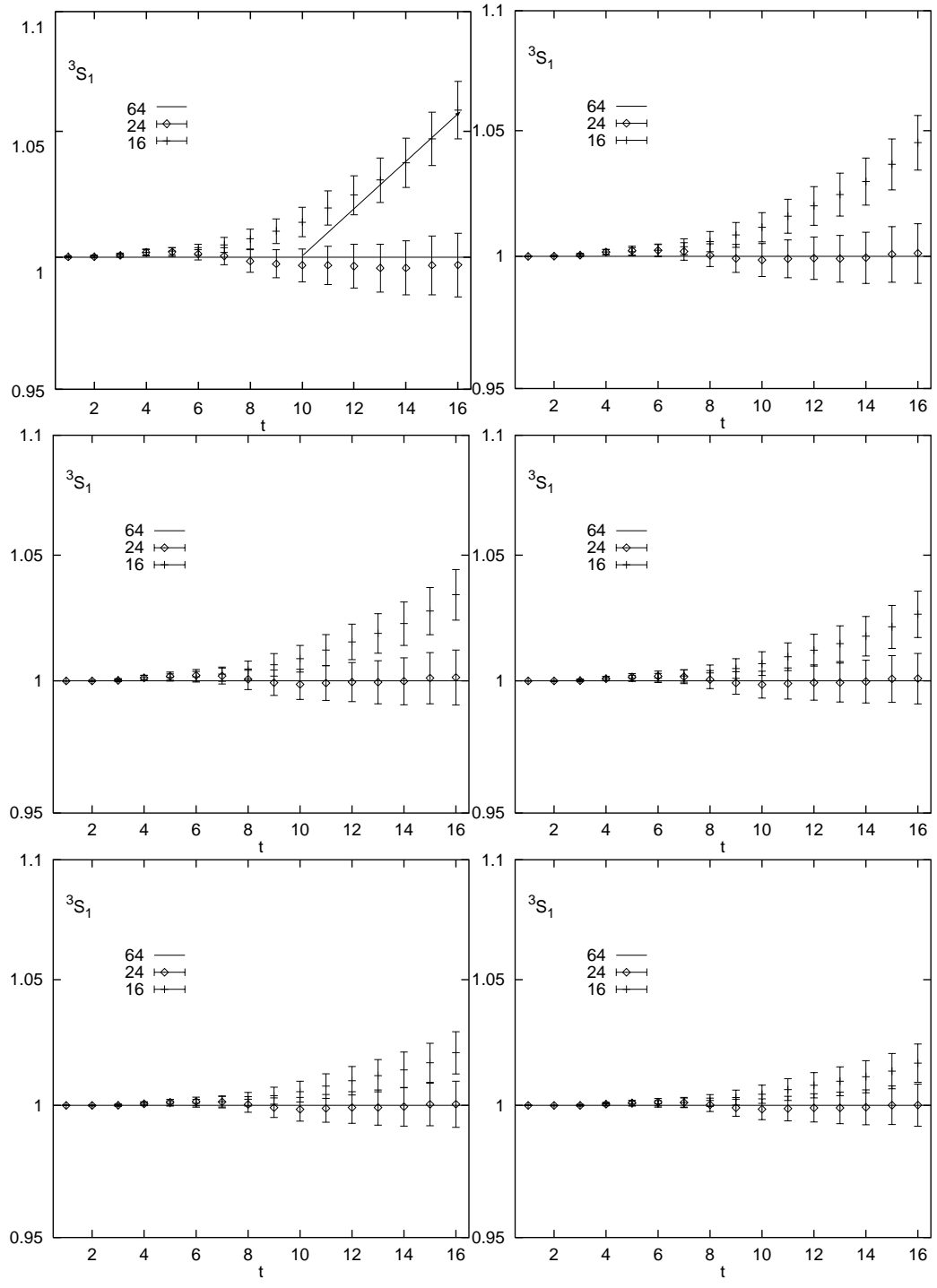


Fig. 6. Scaled local $n=1$ 3S_1 meson propagators $H(T)$ for 6 values of the bare quark mass starting with the lightest mass in the upper left corner on a logarithmic scale.

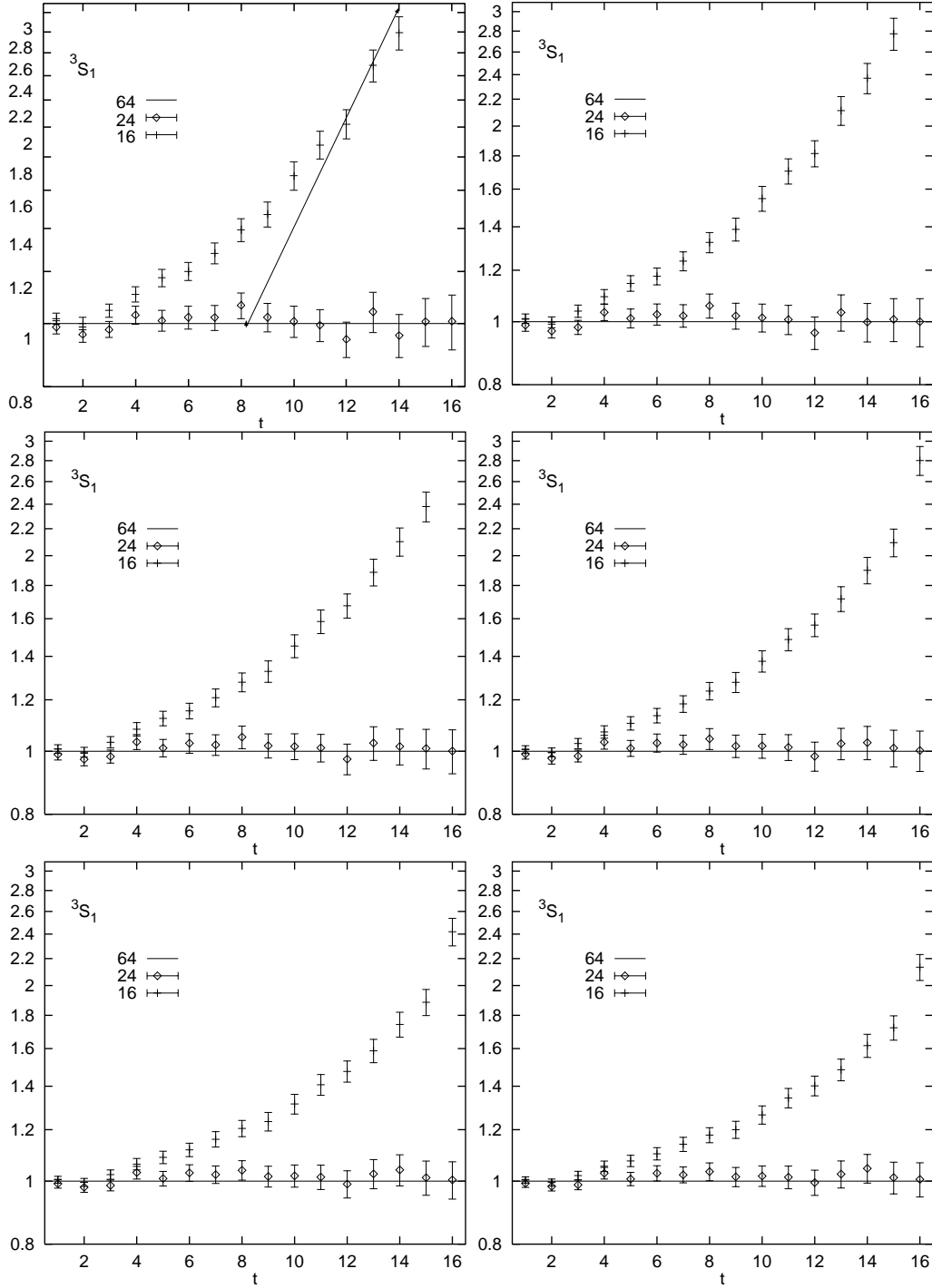


Fig. 7. Scaled smeared-smeared $n=2$ 3S_1 meson propagators $H(T)$ for 6 values of the bare quark mass increasing from upper left to lower right corner on a logarithmic scale.